Monthly Notices
of the
ROYAL ASTRONOMICAL SOCIETY

MNRAS **477,** L90–L95 (2018)
Advance Access publication 2018 March 24

doi:10.1093/mnrasl/sly048

A new ultraluminous X-ray source in the galaxy NGC 5907

F. Pintore,[1★] A. Belfiore,[1] G. Novara,[1,2] R. Salvaterra,[1] M. Marelli,[1] A. De Luca,[1] M. Rigoselli,[1,3] G. Israel,[4] G. Rodriguez,[4] S. Mereghetti,[1] A. Wolter,[5] D. J. Walton,[6] F. Fuerst,[7] E. Ambrosi,[8,9] L. Zampieri,[8] A. Tiengo[1,2] and C. Salvaggio[3]

[1]*INAF – IASF Milano, Via E. Bassini 15, I-20133 Milano, Italy*
[2]*Scuola Universitaria Superiore IUSS Pavia, Piazza della Vittoria 15, I-27100 Pavia, Italy*
[3]*Dipartimento di Fisica, Università degli Studi di Milano-Bicocca, Piazza della Scienza 3, I-20126 Milano, Italy*
[4]*INAF – Osservatorio Astronomico di Roma, Via Frascati 44, I-00040 Monteporzio Catone, Italy*
[5]*INAF – Osservatorio Astronomico di Brera, via Brera 28, I-20121 Milano, Italy*
[6]*Institute of Astronomy, Madingley Road, Cambridge CB3 0HA, UK*
[7]*European Space Astronomy Centre (ESAC), Science Operations Department, E-28692 Villanueva de la Caada, Madrid, Spain*
[8]*INAF – Osservatorio Astronomico di Padova, Vicolo dell'Osservatorio 5, I-35122 Padova, Italy*
[9]*Dipartimento di Fisica e Astronomia, Università degli Studi di Padova, Via VIII Febbraio 1848, 2, I-35122 Padova, Italy*

Accepted 2018 March 22. Received 2018 February 9; in original form 2018 March 21

ABSTRACT

We report on the serendipitous discovery of a new transient in NGC 5907, at a peak luminosity of 6.4×10^{39} erg s^{-1}. The source was undetected in previous 2012 *Chandra* observations with a 3σ upper limit on the luminosity of 1.5×10^{38} erg s^{-1}, implying a flux increase of a factor of >35. We analysed three recent 60 ks/50 ks *Chandra* and 50 ks *XMM–Newton* observations, as well as all the available *Swift/XRT* observations performed between 2017 August and 2018 March. Until the first half of 2017 October, *Swift/XRT* observations did not show any emission from the source. The transient entered the ultraluminous X-ray source (ULX) regime in less than two weeks and its outburst was still on-going at the end of 2018 February. The 0.3–10 keV spectrum is consistent with a single multicolour blackbody disc ($kT \sim 1.5$ keV). The source might be an $\sim$30 M$_\odot$ black hole accreting at the Eddington limit. However, although we did not find evidence of pulsations, we cannot rule out the possibility that this ULX hosts an accreting NS.

Key words: accretion, accretion discs – X-rays: binaries – X-rays: galaxies – X-rays: individual: NGC 5907 ULX-2.

1. INTRODUCTION

Ultraluminous X-ray sources (ULXs; e.g. Kaaret, Feng & Roberts 2017) are a class of extragalactic point-like sources, with X-ray luminosities higher than 10^{39} erg s^{-1} up to, in the most extreme cases, 10^{42} erg s^{-1} (e.g. HLX-1; Farrell et al. 2009). Such luminosities are hence well above the Eddington limit for accretion of pure hydrogen on to a 10 M$_\odot$ black hole (BH). The number of known ULXs is still increasing and nowadays more than 300 sources are confirmed ULXs, as catalogued e.g. by *ROSAT* (Liu & Bregman 2005), *Chandra* (Swartz et al. 2011), and *XMM–Newton* (Walton et al. 2011).

ULXs represent a current hot topic of X-ray astronomy because of their peculiar accretion properties. It is believed that ULXs are accreting compact objects in binary systems (e.g. Motch et al. 2014; Urquhart et al. 2018), but the nature of the compact object is still under debate: indeed ULXs may host either (i) intermediate mass BH (IMBHs, 100–10^5 M$_\odot$; Colbert & Mushotzky 1999) accreting well below the Eddington limit, or (ii) stellar BHs (5 M$_\odot$ < $M_{\rm BH}$ < 80 M$_\odot$; e.g. Gladstone, Roberts & Done 2009; Zampieri & Roberts 2009; Walton et al. 2013; Middleton et al. 2015) or (iii) even neutron stars (NSs), accreting at extremely super-Eddington rates (e.g. Israel et al. 2017a).

However, it is now thought that the vast majority of the ULX population is composed of super-Eddington accreting compact objects. In particular, the presence of NSs in at least four ULXs is confirmed by the detection of pulsation (Bachetti et al. 2014; Israel et al. 2017a,b; Fürst et al. 2016; Carpano et al. 2018). In addition, these pulsating ULXs (PULXs) show significant flux variability of several orders of magnitude. The variety of possible compact objects in ULXs suggests they are a manifold population hosting both BHs and NSs (e.g. Middleton & King 2017), although their relative number is still highly uncertain.

★ E-mail: pintore@iasf-milano.inaf.it

Here we report the discovery of a new X-ray transient in the direction of the galaxy NGC 5907 (Fig. 1), located at a distance of 17.1 Mpc (Tully et al. 2013). NGC 5907 hosts a large population of X-ray sources, with the brightest being the PULX NGC 5907 X-1 (e.g. Sutton et al. 2013; Walton et al. 2016; Israel et al. 2017a). The new source reported here could be the second ULX hosted in this galaxy.

2. DATA REDUCTION

2.1 Chandra

We analysed two *Chandra* ACIS-S archival observations of 2012 February 11 (Obs. ID: 12987, 14391). We also obtained, as Director Discretionary Time (DDT), three ACIS-S observations (Obs.ID: 20830, 20994, 20995) taken on 2017 November 7, 2017 February 28, and 2018 March 1. The Chandra observation exposure times are ∼17, ∼14, ∼52, ∼32, and ∼16 ks, respectively. *Chandra* data were reduced with CIAO v.4.9 and calibration files CALDB v.4.7.6. The source events were chosen from a circular region of radius 3 arcsec, while the background was selected in a circular region of radius 15 arcsec and free of sources. We obtained source spectra with the CIAO task SPECEXTRACT, which creates the appropriate response/auxiliary files for the spectral analysis. With the PILEUP_MAP tool, we estimated that pile-up effects contribute to ∼1 per cent, and we can neglect it. Because of their close temporal proximity, the 2018 observations were analysed as a single data set.

2.2 Swift

We analysed all the available (24) *XRT* observations of the *Neil Gehrels Swift Observatory* taken between 2017 August and 2018 March, with an average exposure time of ∼2 ks. These observations are generally spaced at intervals of about one week. We reduced the data with XRTPIPELINE and extracted 0.3–10 keV light curves selecting circular regions of radii 20 and 130 arcsec for source and background, respectively. We also analysed UVOT data by reducing them with standard procedures.[1]

2.3 *XMM–Newton*

On 2017 December 2, we obtained a DDT *XMM–Newton* observation with a total exposure time of 60 ks. We extracted the data from EPIC-pn and the two EPIC-MOS cameras, and reduced them with SAS v15.0.0. We selected single- and double-pixel events (PATTERN ≤ 4), and single- and multiple-pixel events (PATTERN ≤ 12), for pn and the MOS, respectively. We removed high-background time intervals and we obtained net exposure times of ∼38 ks in the pn and ∼58 ks in the MOS. For spectral and timing analyses, we extracted the source and background events from circular regions of radii 30 and 60 arcsec, respectively.

2.4 *HST*

We analysed optical images of the field collected with the *Hubble Space Telescope* (*HST*). The field was observed with the Wide Field and Planetary Camera 2 (WFPC2) instrument on 1996 March 31 in the *F*450*W* ($\lambda = 4556$ Å, $\Delta\lambda = 951$ Å) and *F*814*W* ($\lambda = 8012$ Å, $\Delta\lambda = 1539$ Å) filters, and on 2007 October 1 in the *F*606*W* filter ($\lambda = 5997$Å, $\Delta\lambda = 1502$Å), with exposure times of 2340, 960, and 3400 s, respectively. We retrieved calibrated, geometrically corrected images from the *Hubble* Legacy Archive (HLA[2]) – such images have an improved astrometry based on cross-correlation with the Sloan Digital Sky Survey catalogue, with r.m.s. accuracy of ∼0.1 arcsec per coordinate. We carried out a source detection using the SExtractor software (Bertin & Arnouts 1996) and we converted count rates to magnitudes in the ST system using the photometric calibration provided by the HLA pipeline.

3. RESULTS

In the 2017 *Chandra* ACIS-S image, we detected a new bright X-ray source that was not present in the same field in the 2012 *Chandra* observation (right inset in Fig. 1). The most precise position of this new transient (ULX-2 hereafter) was obtained with the CIAO task WAVDETECT, which gives coordinates RA $= 15^{\rm h}16^{\rm m}1^{\rm s}.10$ and Dec. $= 56^{\circ}17'51.40"$ (statistical uncertainty of 0.03 arcsec). The source is therefore superimposed on the NGC 5907 galactic plane and at a distance from ULX-1 of ∼28 arcsec.

3.1 Temporal analysis

In the 2012 *Chandra* observations, ULX-2 was not detected, with a 3σ upper limit of 4.4×10^{-15} erg cm^{-2} s^{-1} on the 0.3–10 keV flux (assuming a multicolour blackbody disc, see below). The transient was undetected also in all the *Swift/XRT* observations taken before 2017 October 15. Stacking the August/September observations we obtained a 3σ upper limit of 2.2×10^{-14} erg cm^{-2} s^{-1} on the average flux (shown in Fig. 2-left). A source consistent with the position of ULX-2 was detected in later *Swift/XRT* observations taken at the end of October till the half of 2018 February. Because of the angular resolution of *Swift/XRT* (∼18 arcsec HPD), we cannot exclude that other sources, very close to ULX-2, became active in the same period. However, if we associate the *Swift/XRT* source with ULX-2, these findings suggest that it entered the ULX regime in the second half of 2017 October.

The 0.3–10 keV background-subtracted 2017 *Chandra* light curve of ULX-2 is shown in Fig. 2-right (top panel). A fit with a constant flux gives χ^2/d.o.f. $= 46/10$, indicating the presence of variability (for time-scales >5000 s). On the other hand, we found that, both during the *XMM–Newton* and 2018 *Chandra* observations, the source had a rather constant flux (χ^2/d.o.f. $= 12.1/11$ and χ^2/d.o.f. $= 5.3/6$; Fig. 2-centre, bottom panel). We also investigated, in both *XMM–Newton* and *Chandra* data, the hardness ratio between the energy bands 0.5–1.5 keV (*soft*) and 1.5–10 keV (*hard*) which indicates no significant spectral variability.

We then created a power spectrum (only for the *XMM–Newton* and 2017 *Chandra* observations, because of the too low 2018 *Chandra* counting statistics) for the whole energy band (0.3–10 keV) but we could not find any coherent signal in both data sets. Assuming sinusoidal modulation, we derived a 3σ upper limit on the pulsed fraction (defined as the semi-amplitude of the sinusoid divided by the source average count rate) of 60 and 35 per cent for *Chandra* and *XMM–Newton*, for periods in the range of ∼6–5000 and ∼0.140–150 s, respectively. An accelerated search for coherent signals using a grid of 6234 $\dot{\rm P}$/P values in the range $\pm 10^{-11}$–10^{-6} s s^{-2} gave no statistically significant signals.

[1] http://www.swift.ac.uk/analysis/uvot/index.php

[2] https://hla.stsci.edu/hlaview.html

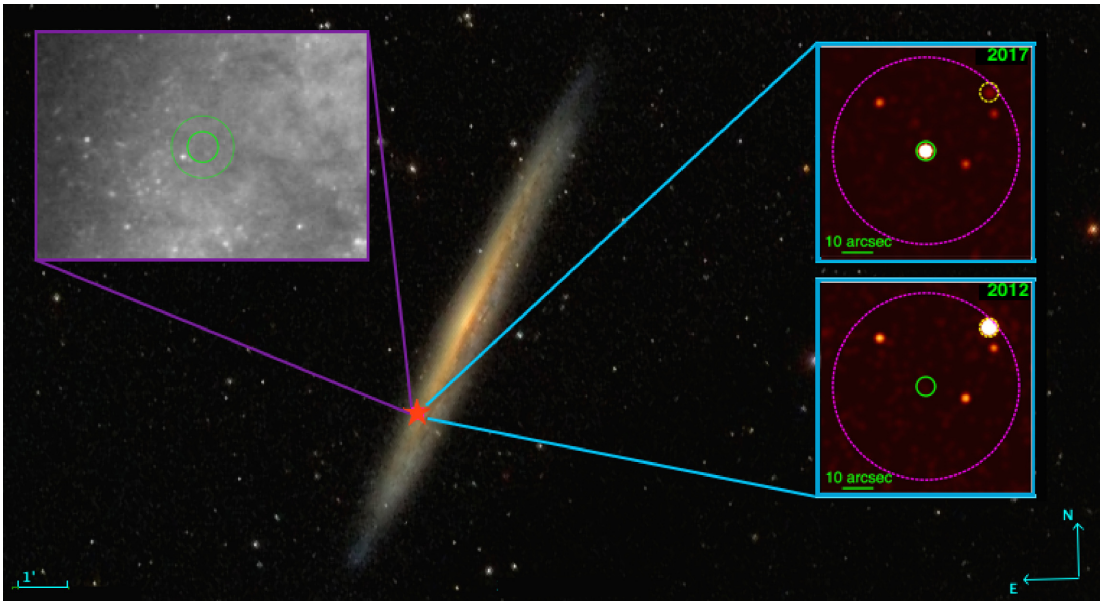

Figure 1. Main figure: SDSS optical image of the galaxy NGC 5907 (north is up); the red star indicates the *Chandra* position of the new ULX transient. Inset box-right: *Chandra* images of the 2012 (bottom) and 2017 (top) observations, where the green, dashed purple, and dashed yellow circles indicate the *Chandra* (3 arcsec radius) and EPIC (30 arcsec radius) extraction regions for the new transient, and the ULX-1 position, respectively. Inset box-left: Archival *HST*/WFPC2 image (15 arcsec × 10 arcsec) of the field of the new transient source NGC 5907 ULX-2 (*F*606*W* filter); ULX-1 is out of image. The green circles mark the X-ray uncertainty region (radius of 0.47 and 1.42 arcsec at 68 per cent and 99 per cent confidence level, respectively) after registering *Chandra* astrometry using a set of SDSS sources. The brightest object within the 99 per cent region (*F*606*W* magnitude of 24.65 ± 0.07, ST system) is the candidate optical counterpart of the transient ULX.

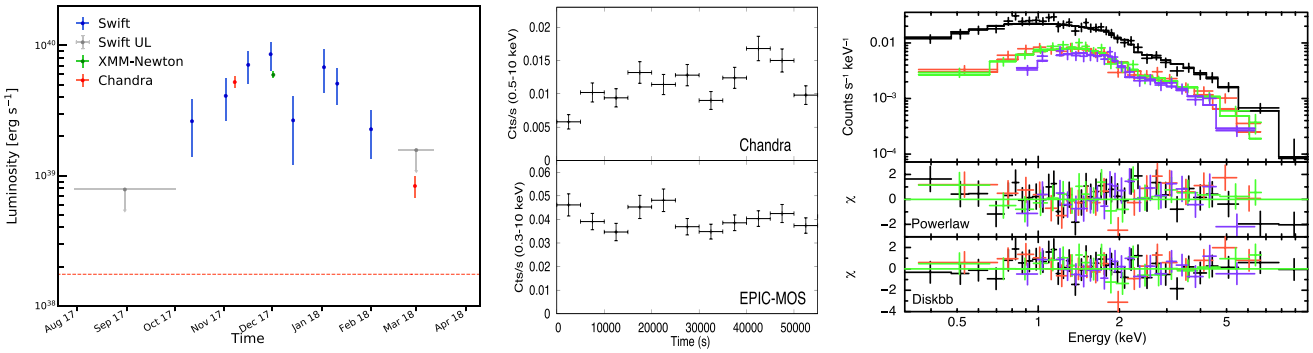

Figure 2. Left: Background-subtracted 0.3–10 keV unabsorbed luminosity light curve of ULX-2; the blue, green, and red points represent the *Swift/XRT* (binning two consecutive observations in each point; errors at 1σ), *Chandra*, and *XMM–Newton* observations (errors at 90 per cent); the grey points are instead the 3σ *Swift/XRT* upper limits (where we assume the EPIC DISKBB best-fitting model) obtained stacking all the observations between 2017 August–September and 2018 February–March; finally, the dashed red line is the 2012 *Chandra* upper limit. **Center**: 2017 *Chandra* (top) and EPIC-MOS (bottom) background-subtracted light curve, binned with 5000 s (to have more than 20 counts in each bin), with the *X*-axis reported to the starting time of each observation. **Right**: Top panel: averaged spectrum of the *XMM–Newton* (black: EPIC-pn, red: EPIC-MOS1, green: EPIC-MOS2) and 2017 *Chandra* (blue) observations, fitted with a DISKBB; middle panel: residuals of the POWERLAW fit; bottom panel: residuals of the DISKBB fit; spectra have been rebinned for display purposes only.

3.2 Spectral analysis

As the hardness ratio does not indicate significant spectral variability in the single observations, we extracted an averaged spectrum for the *XMM–Newton*/EPIC (pn + MOS1/2), and the 2017 and 2018 *Chandra* data; they collect ∼3600, and ∼550 and ∼95 net source counts, respectively. We rebinned the spectra with at least 20 counts per bin and used XSPEC v.12.8.2 to fit them.

We first analysed the EPIC spectra and adopted simple models as a POWERLAW, or a BLACKBODY or a DISKBB, absorbed with TBABS and using the abundances of Wilms, Allen & McCray (2000). We found that acceptable spectral fits ($\chi^2_\nu < 1$) are obtained with the POWERLAW or the DISKBB (Table 1). However, the POWERLAW model left some skewed residuals (in particular above 5 keV, see Fig. 2, right-middle panel). Hence, in the following, we focus on the DISKBB fit (see Fig. 2, right-bottom panel). With the latter, we estimated a mean disc temperature of ∼1.5 keV, a total column density of 8×10^{20} cm^{-2}, hence higher than the Galactic $n_{\rm H}$ along the source direction (1.38×10^{20} cm^{-2}; Dickey & Lockman 1990), and an absorbed 0.3–10 keV flux of $(1.7 \pm 0.1) \times 10^{-13}$ erg cm^{-2} s^{-1}. If ULX-2 is in NGC 5907, the flux translates to an unabsorbed luminosity of $\sim 6.4 \times 10^{39}$ erg s^{-1} (for a distance of 17.1 Mpc).

The 2017 *Chandra* spectrum was then fitted with the DISKBB model with $n_{\rm H}$ fixed to the column density found in the EPIC

Table 1. Best-fitting spectral parameters of the transient source. Errors at 90 per cent confidence level for each parameter of interest.

		XMM–Newton			2017 *Chandra*		2018 *Chandra*		
	$n_{\rm H}$	kT/Γ	Norm.	Flux[a]	kT/Γ	Norm.	kT/Γ	Norm.	χ^2/d.o.f.[b]
	10^{22} cm^{-2}	(keV)		10^{-13} erg cm^{-2} s^{-1}	(keV)		(keV)		
BBODY	<0.8	$0.67^{+0.03}_{-0.03}$	$1.6^{+0.1}_{-0.1}\times10^{-6}$	$1.36^{+0.08}_{-0.08}$	$0.71^{+0.05}_{-0.05}$	$1.3^{+0.1}_{-0.1}\times10^{-6}$	$0.6^{+0.1}_{-0.1}$	$2.3^{+0.5}_{-0.4}\times10^{-7}$	[309/170]
POWERLAW	$0.28^{+0.05}_{-0.04}$	$1.75^{+0.09}_{-0.1}$	$3.9^{+0.4}_{-0.4}\times10^{-5}$	$1.9^{+0.1}_{-0.1}$	$1.9^{+0.1}_{-0.1}$	$3.2^{+0.4}_{-0.4}\times10^{-5}$	$1.9^{+0.4}_{-0.3}$	$5.6^{+1.7}_{-1.5}\times10^{-6}$	**163/170**
DISKBB	$0.08^{+0.03}_{-0.02}$	$1.5^{+0.1}_{-0.1}$	$1.7^{+0.5}_{-0.4}\times10^{-3}$	$1.7^{+0.1}_{-0.1}$	$1.3^{+0.2}_{-0.1}$	$2.2^{+1.1}_{-0.8}\times10^{-3}$	$1.1^{+0.3}_{-0.2}$	$9.1^{+15}_{-5.9}\times10^{-4}$	**162/170**

[a] EPIC absorbed flux in the 0.3–10 keV energy band; [b] as found in EPIC; values in boldface are statistically acceptable.

spectra. The DISKBB provides a very good fit (χ^2/d.o.f. < 1), with a disc temperature consistent within the uncertainties with the EPIC value (Table 1). We note that the average ULX-2 absorbed flux during this *Chandra* observation was ∼20 per cent lower [$(1.2 \pm 0.1) \times 10^{-13}$ erg cm^{-2} s^{-1}] than that found during the *XMM–Newton* observation. However, we also checked that the source flux in the last 20 ks of this *Chandra* observation was consistent with the *XMM–Newton* one. We also note that, inside the *XMM–Newton* source extraction region, at least three other weaker sources are included (as seen in the *Chandra* image). We estimated that they may increase the ULX-2 flux of ≤ 10 per cent and can possibly affect its spectrum but the contaminant effect on the ULX-2 EPIC spectrum appears very marginal because of the strong agreement with the *Chandra* data.

Finally, the 2018 *Chandra* spectrum was still compatible with a DISKBB model (χ^2_ν/d.o.f. $= 5.33/6$, Table 1). Fixing the column density to 8×10^{20} cm^{-2}, we found an inner disc temperature of 1.1 ± 0.3 keV and an absorbed 0.3–10 keV flux of $(2.1 \pm 0.4) \times 10^{-14}$ erg cm^{-2} s^{-1}, i.e. a luminosity of $\sim 7 \times 10^{38}$ erg s^{-1} and thus well below the ULX threshold luminosity.

3.3 Optical data

We searched for an optical counterpart inside the X-ray *Chandra* error circle (radius of 1.3 arcsec). In the archival *HST*/*WFPC2* data observations, we found a bright object (Fig. 1, inset-right) that we consider as the most promising candidate counterpart, with ST magnitudes of 23.7 ± 0.1, 24.65 ± 0.07, and 24.12 ± 0.09 (absolute magnitudes of -7.5 ± 0.1, -6.51 ± 0.07, and -7.04 ± 0.09) in the *F*450*W*, *F*606*W*, and *F*814*W* filters, respectively. Luminosity and colours of this source are consistent with an OB-type star in NGC 5907. We compared the simultaneous *F*450*W* and *F*814*W* measurements with emission models of ULX binaries (Ambrosi & Zampieri, in preparation). The evolutionary tracks of a binary with an ∼20–30 $M_\odot$ BH and an evolved donor with a main sequence mass of ∼20 $M_\odot$ are in agreement with the Galactic extinction corrected photometry, and the mass transfer rate is above Eddington. A detailed modelling is under way and will be presented elsewhere.

4. DISCUSSION

The long-term variability, the $n_{\rm H}$ higher than the Galactic column density and the quite hard X-ray spectrum of the newly discovered source disfavour the identification with a star in our Galaxy. In particular, a foreground star of any spectral type and with the X-ray flux of ULX-2 should have an optical magnitude $M_V < 18$ mag (Krautter et al. 1999). To explore the chance coincidence of a background active galactic nucleus (AGN), we considered the X-ray Log N – Log S of extragalactic sources: the number of AGNs per square degree with a flux larger than $>10^{-13}$ erg cm^{-2} s^{-1} is of the order of a few (e.g. Moretti et al. 2003). For an estimated area of 4.7 arcmin ×0.5 arcmin covered by NGC 5907, this translates on a number of contaminant AGNs less than 5×10^{-3}. We finally rule out the possibility of a supernova event as no significant UV variability has been seen in UVOT data, where, however, the source contribution cannot be distinguished from the rest of the galaxy.

We therefore conclude that the new source is indeed in all respects a ULX transient in NGC 5907, and its peak luminosity is $\sim 6.4 \times 10^{39}$ erg s^{-1}, making this source the second brightest ULX in the galaxy. This implies a luminosity increment of at least a factor of ∼35 with respect to the 2012 *Chandra* upper limit. Before 2017 October, it was below the nominal ULX threshold luminosity ($>10^{39}$ erg s^{-1}) where it returned at the end of 2018 February ($L_X = 7 \times 10^{38}$ erg s^{-1}), following an exponential decay with folding time of 27 ± 4 d. We remark that we could investigate the new source properties with *XMM–Newton* because the close (∼28 arcsec) ULX-1 was in quiescence and hence not contaminating the ULX-2 emission. Although beyond the scope of this paper, we double-checked all the available *XMM–Newton* observations of ULX-1 and, through a Maximum Likelihood analysis based on the EPIC-pn/EPIC-MOS PSFs (e.g. Rigoselli & Mereghetti 2018) we found hints for the presence of ULX-2 only during the observation of 2013 November 6 (at an estimated 0.3–10 keV flux of $\sim 8 \times 10^{-15}$ erg cm^{-2} s^{-1}), when ULX-1 was very weak. However, our analysis does not fully account for possible contaminants close to the ULX-2 position, which may affect the reported flux.

ULX spectra, in the so-called ultraluminous state (Roberts 2007), are generally well described by at least two spectral components interpreted as a soft thermal emission ($kT \sim 0.1-0.5$ keV) from cold optically thick outflows and hard thermal emission from a hot modified accretion disc or corona close to the compact object (e.g. Gladstone, Roberts & Done 2009; Pintore & Zampieri 2012; Sutton, Roberts & Middleton 2013; Bachetti et al. 2014; Middleton et al. 2015; Walton et al. 2016). On the other hand, there is a small sample of ULXs with very limited data quality displaying properties consistent with the spectral states of Galactic accreting BHs X-ray binaries (Sutton et al. 2012). However, some of these ULXs showed the features of the Ultraluminous state when data of better quality became available (e.g. Sutton et al. 2013; Pintore et al. 2016). We believe that this is not the case for ULX-2 because the quality of its current spectra is relatively good (∼3500 net EPIC counts).

We found that the average ULX-2 spectrum is described by a single multicolour accretion disc with a temperature of ∼1.5 keV, indicating that the source may be in a *soft* state reminiscent of those found in Galactic accreting BH binaries (e.g. McClintock & Remillard 2006). However, although not supported by the data, we cannot exclude that its disk-like shape might suggest that ULX-2 is in the super-Eddington 'very thick state' (i.e. a spectral shape consistent with Comtponization from an optically thick corona with $\tau > 10$ and $kT_e \sim 1$–2 keV; see Pintore & Zampieri 2012). In any case, if the source is radiating close to the Eddington limit (and we consider the *soft* state as reliable), the implied mass would be $M_{BH} \sim L_X/(1.38 \times 10^{38})M_\odot \sim 30\ M_\odot$ (assuming isotropic emission). Although the mass of such an object would be larger than any accreting BH found in our Galaxy, the LIGO and VIRGO detectors showed the existence of BHs of similar sizes (Abbott et al. 2016, 2017). Assuming an inclination angle $<70^\circ$ (because of the absence of dips or eclipses), the best-fitting DISKBB normalization corresponds to an estimated inner accretion disc radius of <140 km, or to an upper limit of $\sim 15\ M_\odot$ for the mass of a non-rotating BH (Lorenzin & Zampieri 2009). In addition, although the error bars are large, we note that the relation $L_X \propto kT_{disc}^4$ (valid for a standard accretion disc) is compatible with our temperature and luminosity values.

Until now, only a handful of transient ULXs are known and not all of them have been deeply studied. Some examples of ULX transients are M31 ULX-1 and ULX-2 (e.g. Middleton et al. 2012; Esposito et al. 2013; Middleton et al. 2013), three ULXs in the Cartwheel galaxy (Crivellari, Wolter & Trinchieri 2009), CXOU 133705.1−295207 in M83 (Soria et al. 2012), CXOU J132518.2−430304 in NGC 5128 (Sivakoff et al. 2008) and M82 X-1. Their outbursts can be explained, for instance, in terms of an unstable mass transfer from the companion star. The three PULXs – M82 X-2 (e.g. Bachetti et al. 2013), NGC 7793 X-1 (Motch et al. 2014), and NGC 5907 ULX-1 (e.g. Walton et al. 2015) – from time to time also show high flux variability of several orders of magnitude, which may be explained by the onset/switch-off of the propeller stage. The flux variability of at least a factor of ∼40 between high and low flux states of ULX-2 is similar to that ascribed to the propeller effects in M82 X-2 (see e.g. Tsygankov et al. 2016). We did not find any coherent pulsations in ULX-2 with an upper limit on the pulsed fraction of 35 per cent. Only the pulsed fraction of NGC 300 ULX-1 is larger than this value, while the other three PULXs have smaller modulations. Thus, we cannot exclude that ULX-2 hosts a NS accreting at very high rates although, from a spectral point of view, it may be slightly softer than the PULXs (e.g. Pintore et al. 2017; Walton et al. 2018). Furthermore, all the PULXs show superorbital modulations that the available data do not allow us to search. But a deeper monitoring with *Swift* or *XMM–Newton* (during the quiescence of ULX-1) or, even better, with *Chandra* could provide indications about superorbital modulations.

The *HST* image indicates that the source might have an optical counterpart with the colours of an OB type star. Only ∼20 ULX optical counterparts have been identified (Tao et al. 2011; Gladstone et al. 2013) and, when individual optical counterparts can be associated with a ULX, they often appear to have the luminosities and colours of OB type giants or supergiants (e.g. Zampieri et al. 2004; Soria et al. 2005), even though the disc emission may contribute significantly to the optical flux (Patruno & Zampieri 2008). New optical observations are strongly needed to constrain the nature of the ULX-2 counterpart.

ACKNOWLEDGEMENTS

We thank Dr. B. Wilkes, Dr. N. Schartel, and Dr. Brad Chenko who made the *Chandra*, *XMM–Newton*, and the *Neil Gehrels Swift Observatory* DDT observations possible.

This work is based on NASA/ESA Hubble Space Telescope observations and obtained from the Hubble Legacy Archive.

DJW acknowledges support from STFC in the form of an Ernest Rutherford fellowship. We acknowledge financial support from the Italian National Institute for Astrophysics (INAF) through the project 'ACDC – ASTRI/CTA Data Challenge', from the Italian Space Agency (ASI) through the ASI-INAF agreements 2015-023-R.0 and 2017-14-H.0, as well as from the EXTraS project ('Exploring the X-ray Transient and variable Sky'), funded from the EU's 17th Framework Programme under grant agreement no. 607452, and the high performance computing resources and support provided by the CINECA (MARCONI) and by the INAF – CHIPP.

REFERENCES

Abbott B. P. et al., 2016, Phys. Rev. Lett., 116, 061102
Abbott B. P. et al., 2017, Phys. Rev. Lett., 118, 221101
Bachetti M. et al., 2013, ApJ, 778, 163
Bachetti M. et al., 2014, Nature, 514, 202
Bertin E. , Arnouts S., 1996, A&AS, 117, 393
Carpano S., Haberl F., Vasilopoulos G., Maitra C., 2018, MNRAS, 476, 45C
Colbert E. J. M., Mushotzky R. F., 1999, ApJ, 519, 89
Crivellari E. , Wolter A., Trinchieri G., 2009, A&A, 501, 445
Dickey J. M. , Lockman F. J., 1990, ARA&A, 28, 215
Esposito P., Motta S. E., Pintore F., Zampieri L., Tomasella L., 2013, MNRAS, 428, 2480
Farrell S. A., Webb N. A., Barret D., Godet O., Rodrigues J. M., 2009, Nature, 460, 73
Fürst F. et al., 2016, ApJ, 831, L14
Gladstone J. C., Roberts T. P., Done C., 2009, MNRAS, 397, 1836
Gladstone J. C., Copperwheat C., Heinke C. O., Roberts T. P., Cartwright T. F., Levan A. J., Goad M. R., 2013, ApJS, 206, 14
Israel G. L. et al., 2017a, Science, 355, 817
Israel G. L. et al., 2017b, MNRAS, 466, L48
Kaaret P., Feng H., Roberts T. P., 2017, ARA&A, 55, 303
Krautter J. et al., 1999, A&A, 350, 743
Liu J.-F., Bregman J. N., 2005, ApJS, 157, 59
Lorenzin A., Zampieri L., 2009, MNRAS, 394, 1588
McClintock J. E., Remillard R. A., 2006, in Levin W. H. G., der Klis van M., eds, Compact Stellar X-ray Sources. Cambridge Univ. Press, Cambridge, p. 157
Middleton M. J., King A., 2017, MNRAS, 470, L69
Middleton M. J., Sutton A. D., Roberts T. P., Jackson F. E., Done C., 2012, MNRAS, 420, 2969
Middleton M. J. et al., 2013, Nature, 493, 187
Middleton M. J., Heil L., Pintore F., Walton D. J., Roberts T. P., 2015, MNRAS, 447, 3243
Moretti A., Campana S., Lazzati D., Tagliaferri G., 2003, ApJ, 588, 696
Motch C., Pakull M. W., Soria R., Grisé F., Pietrzyński G., 2014, Nature, 514, 198
Patruno A., Zampieri L., 2008, MNRAS, 386, 543
Pintore F., Zampieri L., 2012, MNRAS, 420, 1107
Pintore F., Zampieri L., Sutton A. D., Roberts T. P., Middleton M. J., Gladstone J. C., 2016, MNRAS, 459, 455
Pintore F., Zampieri L., Stella L., Wolter A., Mereghetti S., Israel G. L., 2017, ApJ, 836, 113
Rigoselli M., Mereghetti S., 2018, preprint (arXiv:1802.09454)
Roberts T. P., 2007, Ap&SS, 311, 203
Sivakoff G. R. et al., 2008, ApJ, 677, L27
Soria R., Cropper M., Pakull M., Mushotzky R., Wu K., 2005, MNRAS, 356, 12

Soria R., Kuntz K. D., Winkler P. F., Blair W. P., Long K. S., Plucinsky P. P., Whitmore B. C., 2012, ApJ, 750, 152
Sutton A. D., Roberts T. P., Walton D. J., Gladstone J. C., Scott A. E., 2012, MNRAS, 423, 1154
Sutton A. D., Roberts T. P., Gladstone J. C., Farrell S. A., Reilly E., Goad M. R., Gehrels N., 2013, MNRAS, 434, 1702
Sutton A. D., Roberts T. P., Middleton M. J., 2013, MNRAS, 435, 1758
Swartz D. A., Soria R., Tennant A. F., Yukita M., 2011, ApJ, 741, 49
Tao L., Feng H., Grisé F., Kaaret P., 2011, ApJ, 737, 81
Tsygankov S., Mushtukov A., Suleimanov V., Poutanen J., 2016, MNRAS, 457, 1101
Tully R. B. et al., 2013, AJ, 146, 86
Urquhart R. et al., 2018, MNRAS, 475, 3561U
Walton D. J., Roberts T. P., Mateos S., Heard V., 2011, MNRAS, 416, 1844
Walton D. J., Miller J. M., Harrison F. A., Fabian A. C., Roberts T. P., Middleton M. J., Reis R. C., 2013, ApJ, 773, L9
Walton D. J. et al., 2015, ApJ, 799, 122
Walton D. J. et al., 2016, ApJ, 827, L13
Walton D. J. et al., 2018, MNRAS, 473, 4360
Wilms J., Allen A., McCray R., 2000, ApJ, 542, 914
Zampieri L., Roberts T. P., 2009, MNRAS, 400, 677
Zampieri L., Mucciarelli P., Falomo R., Kaaret P., Di Stefano R., Turolla R., Chieregato M., Treves A., 2004, ApJ, 603, 523

This paper has been typeset from a TEX/LATEX file prepared by the author.